IJE TRANSACTIONS A: Basics Vol. 34, No. 7, (July 2021) 1785-1798

International Journal of Engineering

Journal Homepage: www.ije.ir

Multi-objective Optimal Design of Gas-fired Heater Based on Modified Design Model of Fired Heater Taking into Account Exergy, Economic and Environmental Factors

S. M. Ebrahimi Saryazdi*[a,b], F. Rezaei[a], Y. Saboohi[a], F. Sassani[b]

[a] *Energy Engineering Department, Sharif University of Technology, Azadi Ave., Tehran, Iran*
[b] *Mechanical Engineering Department, University of British Columbia, Vancouver, BC, Canada*

PAPER INFO

Paper history:
Received 15 February 2021
Received in revised form 31March 2021
Accepted 01 April 2021

Keywords:
Mathematical Model
Gas Fired Heater
Multi-objective Optimization
Exergy Analysis
Environment
Gas Reduction Station

ABSTRACT

Heaters are one of the central parts of natural gas reduction stations using turboexpanders to prevent the formation of hydrate and corrosion failure. This study intends to design a fired heater by applying a combustion sub-model to derive an optimal model for this kind of application. This model is developed to accurately consider all subsections of the fired heater namely radiation, convection, and shield sections, as well as flue gas composition, and its volume. Within this context, a multi-objective optimization is employed to identify the optimal design of the gas-fired heater in the natural gas reduction station for the Ramin power plant case study. The total economic and environmental costs, together with modified exergy efficiency, are selected as objective functions. Multi-criteria-decision-making-method is employed on Pareto frontiers optimal curve to suggest the optimal solution. Results show that the developed model can outperform previous models in thermal efficiency with relatively similar costs. Besides, the optimal point in Pareto suggested by the decision-making-method accounts for a higher modified exergy efficiency (1.3%) than the counterpart, which thermal efficiency is regarded as an objective function. At the same time, its total cost remained almost constant. The effects of changes in each of the design parameters on the objective functions are also evaluated.

***doi**: 10.5829/ije.2021.34.07a.23*

*

NOMENCLATURE

a_1, a_2	Volume of air components	*TAD*	Adiabatic temperature of combustion [K]
A	Heat transfer area [m^2]	*TRE*	Real temperature of combustion [K]
AAS	Air to fuel ratio [–]	U_c	Overall heat transfer coefficient of convection section [w/m^2k]
$Air_{\min}$	Minimum air volume for fuel combustion	v_w	Wind speed [m/s]
B	Constant parameter	*V*	Volume of flue gases [m^3]
c_{cost}	Unitary cost [$/$m^2$]	x_k	Molar fraction of component k in the flue gas [%]
c_{ele}	Electricity price [$/kWh]	*W*	Width of fired heater [m]
c_{CO_2}	Penalty cost of CO_2 emission [$/kg]	**Abbreviations**	
c_{SO_2}	Penalty cost of SO_2 emission [$/kg]	CRF	Capital Recovery Factor
C	Carbon mass percentage in fuel [ppm], Cost [$], Constant parameter	GA	Genetic Algorithm
CO	CO mass percentage in flue gas [ppm]	HTRI	Heat Transfer Research Inc.

* Corresponding Author Institutional Email: ebrahimi@energy.sharif.edu (S. M. Ebrahimi Saryazdi)

Please cite this article as: S. M. Ebrahimi Saryazdi, F. Rezaei, Y. Saboohi, F. Sassani, Multi-objective Optimal Design of Gas-fired Heater Based on Modified Design Model of Fired Heater Taking into Account Exergy, Economic and Environmental Factors, International Journal of Engineering, Transactions A: Basics Vol. 34, No. 7, (2021) 1785-1798

CO_2	CO_2 mass percentage in flue gas [ppm]
$C_{p,dg}$	Heat capacity of fuel [J/kg]
d	Distance $[m]$, Diameter $[m]$
d_{i+}	Distance of point ith from the ideal point
D	Constant parameter
e	Standard molar exergy [J/mole]
ex	Specific exergy [J/kg]
Ex	Exergy [W]
EC	Equilibrium constant of reaction
f	Fanning friction factor [-]
$f_1, f_2, f_3, f_4, f_5, f_6, f_7, f_8, f_9, f_{10}, f_{11}, f_{12}, f_{13}$	Volume of fuel components
F_{ij}	Points of the Pareto frontier
F_{ij}^{n}	Non-dimensionalized objective
F_j^{ideal}	Ideal value for jth objective
G	Mass velocity of hot water
GCV	Gross Calorific Value of fuel [J/kg]
h	Annual operating time [h/y], Specific enthalpy [kJ/kg]
HF	Humidity factor
H_2	Hydrogen mass percentage in fuel [%]
H	Height of fired heater [m]
i	Annual discount rate [%]
k_1	Numerical constant
k_2	Numerical constant
kk_1	Distance between the centers of the end tube and the wall [–]
$L_1, L_2, L_3, L_4, L_5, L_6$	Losses parameters [W]
L	Length [m]
LHV	Lower heating value of fuel [J/kg]
$LMTD$	Logarithmic mean temperature difference [K]
m	Mass flow rate [kg/s]
M_{dg}	Mass of flue gases in kg/kg fuel
M_{moist}	Moisture mass percentage [%]
n	Number of years, Number of point on Pareto frontier, Mole of flue gas [mole]
N_t	Number of tubes
o_{cost}	Fuel unit cost
Q_A	Heat absorbed by the process fluid [W]
Q_{conv}	Heat absorbed in convection section [W]
Q_f	Heat liberated by combustion [W]
Q_{rad}	Heat absorbed in radiation section [W]
Q_{shld}	Heat absorbed in shield section [W]
Q_L	Heat duty [W]

LINMAP	Linear Programming Technique for Multidimensional Analysis of Preference
MINLP	Mixed-Integer Nonlinear Programming
MCDM	Multi-Criteria Decision-Making
REFPROP	Reference Fluid Thermodynamic and Transport Properties Database

Greek Letters

α	Relative effectiveness factor of the tubes bank [-]
η_{exe}	Modified exergy efficiency [-]
η_{comb}	Combustion efficiency [-]
η_{FH}	Fired heater thermal efficiency [-]
η_p	Pump efficiency [-]
v	Mean specific volume of hot water [m^3/kg]
ξ	Constant value
ρ	Density [kg/m^3]
σ	Stefan-Boltzman constant $= 2.041\times10^{-7}\left[kJ/m^2\cdot K^4\cdot h\right]$

Subscripts

air	Air
cc	Distance between the centers of the two tubes side by side
$conv$	Convection section
cp	Plane area of tubes bank
e	Equivalent length
env	Environmental emission
$firebox$	Firebox section
$flue$	Flue gases
$fuel$	Fuel
F	Feed
FH	Fired heater
g	Effective gas temperature in firebox
i	Inlet, Inside, ith point
k	Component k of flue gases
ng	Natural gas
o	Outlet, Outside
opr	Operation
P	Product
rad	Radiation section
$radc$	Ceiling tubes in radiation section
s	Stack
$shld$	Shield section
$total$	Total
w	Water
W	Wall

r_{cost}	Unitary cost [\$/m^2]	0	Ambient state
$\bar{R}$	Universal gas constant, 8.314 [J/kg·K]	**Superscripts**	
s	Specific entropy [J/kg·K]	ch	Chemical
S_i	Heat surface area of each tube in the convection section[m^2]	ph	Physical
T	Temperature [K]	UN	Unavoidable

1. INTRODUCTION

Over 69% of natural gas is transported from wells to consumers through transmission pipelines [1], known as an economical way to transport natural gas across large distances [2]. Besides that, Iran has 11th place globally in the total length of natural gas pipelines [1]. Natural gas pressure should be increased in gas compression stations to overcome friction and heat losses through the natural gas pipeline, and then decreased in gas reduction stations to the desired values [3]. Iran has 2500 gas reduction stations [3], which traditionally consist of a gas-fired heater, throttling valve, heat exchanger, and control system. The pressure reduction in the gas reduction station results in a drop in temperature because of the positive Joule-Thompson coefficient [4] and consequent formation of hydrates. Thus, the preheating system regulates the outlet temperature of natural gas from the turboexpander or throttling valve to provide appropriate means of preventing the formation of hydrate and corrosion failure [5].

As mentioned earlier, gas-fired heaters are one of the central parts of natural gas reduction stations to prevent the formation of hydrate and corrosion failure, especially when a turbo-expander is implemented instead of a pressure reduction valve. Gas-fired heaters [6] or bath-type heaters [7] are commonly employed in natural gas reduction stations. These two types of preheaters burn a remarkable portion of the passing natural gas and have low energy efficiency [7, 8].

With regard to gas reduction station preheating system, the focus of recent research has been on replacing the conventional preheating system with novel preheating systems such as solar systems [3, 9], geothermal systems [10], combined heat and power systems (with gas turbine [11], internal combustion engines [12, 13], and Molten-carbonate fuel cells [14] as a prime mover), and thermoelectric generator [15].

Darabi et al. [14] indicated that employing a hybrid turboexpander-fuel cell in gas pressure reduction stations is presently uneconomical. Farzaneh-Gord et al. [16] analyzed the impact of a number of solar collectors with a storage tank on gas reduction stations. According to their economic assessment, the payback ratio was 11 years. Ghezelbash et al. [10] studied the use of vertical ground-coupled heat pumps in gas reduction stations equipped with turboexpander. In this configuration, the ground heat pump preheats the natural gas to reduce fuel consumption of bath-type heaters up to 45.8% annually with a payback period of 6 years.

To the authors' best of knowledge, in recent years, there has been growing interest in the economic and exergy assessment of novel preheating configurations replacing fired heaters with renewable heating systems and novel-heating technologies. Results of previous studies indicated that renewable heating systems and novel-heating technologies are not cost-effective solutions. However, previous studies failed to address the optimal detailed design of the fired heater. Therefore, this paper will focus on the optimal design of fired heaters in gas reduction stations.

A fired heater or tubular heater is a combustion furnace where combustion gases heat the fluids inside the tube. The main advantages of this equipment are having continuous performance and a reduction in foam formation. The oil, gas, and chemical process industries have widely applied this equipment for the heating purposes [17]. Fired heaters consist of three sections, namely radiation (which is also called combustion chamber), convection, and shield section, see Figure 1. The hot combustion gases produced in the radiation section pass through the shield and then convection sections. The shield section, which consists of two/three rows of bare tubes, is located between the other two parts and prevents direct radiation to the convection tubes. The flue gases circulate through a staggered convection tube bundle to increase the heat transfer rate before discharging to the atmosphere. Corbels fill the space between the convection tube and sidewall to prevent flue gas bypass flow [18]. Regarding the geometrical configuration of the radiation section, this equipment is classified as vertical cylindrical or box-type heaters. The last one, which is considered in this study, is typically applied in enormous heat demands. It should be mentioned that tube size and the number of passes of radiation, shield, and convection sections are determined based on the application and fluid flow rate [19].

Various mathematical models have been proposed to simulate the performance of fired heaters. In this regard, Ebrahimi et al. [20] developed the multi-zone mathematical model to simulate the performance of the furnace. Previous studies indicated that solving the matrices in calculating the total heat exchange area limited the application of this model [21]. Ibrahim and Al-Qassimi [22] developed a model to simulate a box-

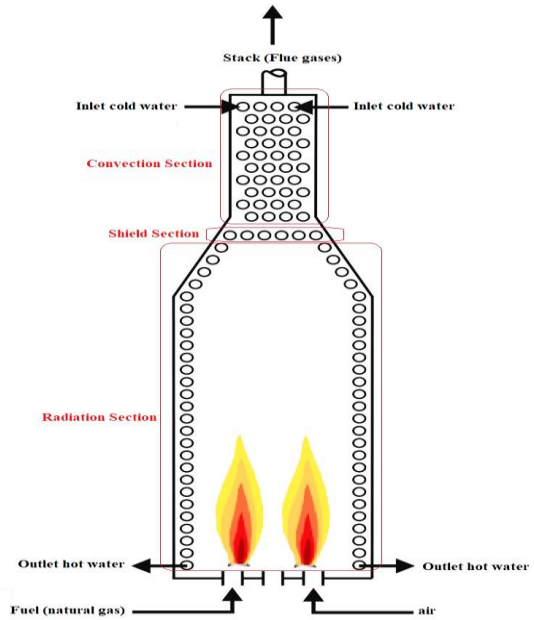

Figure 1. Schematic of fired heater sections

type fired heater in a crude oil atmospheric topping unit. In this study, temperature profile and heat abortion per layer in the convection section were calculated and used to assess this section. Ibrahim and Al-Qassimi [17] studied direct and indirect methods to calculate heater efficiency and indicated that the direct approach has less computational time. Recently, findings regarding fired heaters have led to improve the process operations; however, little attention has been paid to optimize their design. Limitations such as the maximum allowable absorption rate in the radiation section, the maximum permissible pressure drop of heater fluid flow, and so on considerably affect optimal geometry and combustion conditions of the fired heater. Concerning the optimal design of fired heaters, Heat Transfer Research Inc. (HTRI) and Aspen Technology Inc. proposed comprehensive optimal design producers [23]. Moreover, there are century-old standards, such as the standards of the American Petroleum Institute (API) standard 530 [24] and 560 [25], which describe design calculation procedures of fired heaters. Mussati et al. [26] proposed a mathematical model to obtain the optimal design of the fired heater using Mixed-Integer Nonlinear Programming (MINLP). In this study, sensitivity analysis of fuel cost and capital investment cost is carried out. Several case studies were considered, and their optimal design results indicate improvements in economic and operative performances. Haratian et al. [27] optimized box-type fired heater by developing a mathematical model associated with the genetic algorithm (GA). They applied the modified total cost as an objective function by including the pumping cost. Their results have an acceptable accuracy with literature and showed that total cost could decrease up to nearly 2.5% compared to the original design.

Previous studies have not considered the combustion process in their mathematical model of the fired heater, and have assumed the combustion efficiency to be constant [26, 27]. Moreover, these studies have employed a direct method in their design model to calculate thermal efficiency, which depends on stack temperature and excess air fraction. The accuracy of mentioned methods for predicting thermal efficiency subsides with increased stack temperature and excess air fraction [28]. Therefore, the novelty of this work is to propose a new design model of fired heaters associated with the combustion sub-model. An indirect method (heat loss method) integrated with the combustion model is also employed to predict the thermal efficiency of the fired heater through an iterative design process. The optimal design of fired heaters, especially for oil industry applications using total economic cost as an objective function, has attracted much attention in recent years. However, the optimal design of the fired heater of the gas reduction station has not been investigated. With this in mind, the gas reduction station of the Ramin power plant in Iran was selected as a case study. Previous studies also indicated that exergy analysis could be a powerful tool for designing and optimizing processes [29-32]. Therefore, multi-objective optimization of fired heaters applying total economic and environmental cost along with modified exergy efficiency as objective functions are proposed in this study. The environmental cost is integrated with economic costs of fired heater to include emissions of CO_2 and SO_2 pollutants in the fired heater design process. For decision variables, the outlet hot water temperature, the external diameter of tube in radiation as well as convection sections, number of wall-side tubes as well as the ceiling in radiation section, and excess air ratio are considered for the first time in optimal design progress of fired heater due to natural-gas reduction station conditions.

As the initial step, a mathematical model of the box-type fired heater and the combustion process sub-model are developed (section 2.1.1). In this study, the combustion sub-model is applied to obtain the composition and volume of flue gases (section 2.1.2). Then, the fired heater's optimal design is derived using a multi-objective GA (section 2.2). The multi-criteria-decision-making method (MCDM) is employed to obtain an optimal point of the Pareto-frontier and facilitate decision-making, which is generally dependent upon engineering experiences and objective function. Eventually, the variations of objective functions with decision variables are presented in section 3. Given the above, the main contributions of this study are:

- Employing a multi-objective optimization for the optimal design of fired heater in pre-heating natural gas entering the gas-pressure reduction station. Total cost and modified exergy efficiency are both considered objective functions. The environmental cost is also added to the total cost of the fired heater.
- Proposing a modified design model of the fired heater and its diverse sections, including radiation, convection, and shield, etc. Moreover, the geometric structure, dimensions, the number of required tubes, thermal efficiency, and losses are estimated by applying the indirect method and using the combustion sub-model.

2. MODELLING

The flow chart for the optimal design of the fired heater is shown in Figure 2. In the present project, the genetic algorithm (GA) is used to optimize fired heater design. In the first step, GA parameters (Table 1), decision variables (Table 2), and objective functions are determined (which are presented in section 2.2). Then, a mathematical model of the fired heater and sub-model of combustion, which are developed in MATLAB environment, are employed to design all subsections of the fired heater (radiant, shield, convection, and chamber) and to achieve performance parameters of fired heater. The combustion sub-model is provided in section 2.1.2. Inputs of combustion model include fuel and air composition, excess air, fuel and air temperature, air humidity, and air pressure. Combustion sub-model is employed to calculate thermal efficiency (section 2.1.1) and environmental cost (section 2.2.1). Reference Fluid Thermodynamic and Transport Properties Database (REFPROP) database is applied to achieve thermodynamic properties of fluids in these sub-models [33]. A new generation is produced by employing selection, mutation, and crossover operators to evaluate each generation's objective functions. Eventually, the MCDM method (Linear Programming Technique for Multidimensional Analysis of Preference (LINMAP)) is applied to suggest an optimal Pareto Front solution [34]. The formulation of the LINMAP method is presented in Appendix A.

2. 1. Mathematical Model

2. 1. 1. Fired Heater Sub-model The total heat transferred from the radiant and convection sections is calculated from Equation (1).

$$Q_A = m_w \cdot \left(h_{w,o} - h_{w,i}\right) = Q_{rad} + Q_{conv} + Q_{shld} \quad (1)$$

where, Q_{rad}, Q_{conv}, and Q_{shld} refer to the heat transfer rate absorbed in the radiation, convection, and shield sections, respectively.

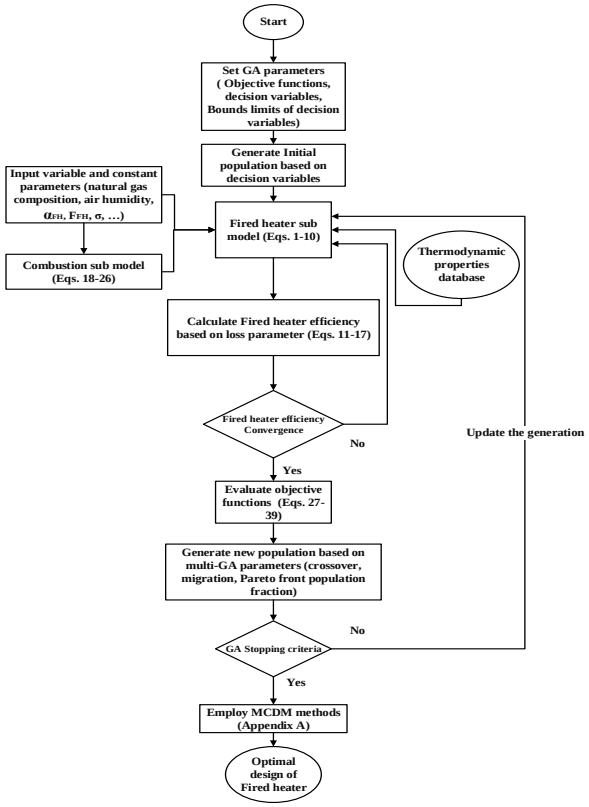

Figure 2. Flow chart of fired heater design and performance model

The amount of heat transferred in the radiation section is the function of the plane area of tubes bank (A_{cp}), effective gas temperature in firebox (T_g), and wall temperature (T_W) [17]:

$$Q_{rad} = \sigma \cdot \left(\alpha \cdot A_{cp}\right) \cdot F \cdot \left(T_g^4 - T_W^4\right) \quad (2)$$

$$A_{cp} = N_{t,rad,total} \cdot d_{cc} \cdot L_{rad} \quad (3)$$

The amount of heat transferred in the shield section is presented in Equation (4) [17]:

$$Q_{shld} = \sigma \cdot \left(\alpha \cdot A_{cp,shld}\right) \cdot F \cdot \left(T_g^4 - T_W^4\right) \quad (4)$$

$$A_{cp,shld} = N_{t,shld} \cdot d_{cc} \cdot L_{rad} \quad (5)$$

Then, the heat balance equation is derives based on Equations (1), (2), and (4). The Newton-Raphson method was used to solve this equation and determine the effective gas temperature (T_g).

$$F\left(T_g\right) = C \cdot T_g^4 + D \cdot T_g - B \quad (6)$$

The constants *C*, *D*, and *B* are determined by fuel type, percentage of excess air, operating conditions, and the fired heater's geometric characteristics. The number of tubes required in the convection section is obtained by Equation (7) [17]:

$$N_{t,conv} = \left(\frac{Q_{conv}}{U_c \cdot LMTD \cdot S_i} \right) \tag{7}$$

The geometric dimension of the heater is defined as Equations (8) and (9):

$$H = \left(\frac{N_{t,rad}}{2} - 1 \right) \cdot d_{cc} + kk_1 \tag{8}$$

$$W \geq \left(\frac{N_{t,radc}}{2} - 1 \right) \cdot d_{cc} + kk_1 \tag{9}$$

The net released heat required in the combustion section is obtained by the heater efficiency (Equation (10)):

$$\eta_{FH} = Q_A / Q_L \tag{10}$$

The difference between the amount of heat absorbed and released by combustion is equal to the sum of the heat losses (Equation (11)):

$$Q_L = Q_A + \sum_{i=1}^{6} L_i \tag{11}$$

where *L* refers to different types of losses that are represented from Equations (12)-(17) [22]:

$$L_1 = 100 \cdot M_{dg} \cdot C_{p,dg} \cdot (T_s - T_{air}) \tag{12}$$

$$L_2 = 900 \cdot H_2 \cdot \left(2445.21 + \left(1.88 \cdot (T_s - T_{air}) \right) \right) \tag{13}$$

$$L_3 = 188 \cdot HF \cdot AAS \cdot (T_s - T_{air}) \tag{14}$$

$$L_4 = 100 \cdot M_{moist,fuel} \cdot \left(2445.21 + \left(1.88 \cdot (T_s - T_{air}) \right) \right) \tag{15}$$

$$L_5 = 100 \cdot \left(\frac{CO}{CO + CO_2} \cdot 24656000 \cdot C \right) \tag{16}$$

$$L_6 = 54.8 \cdot \left(\left(T_W / 55.55 \right)^4 - \left(T_{air} / 55.55 \right)^4 \right) + \left(1.957 \cdot \left(\frac{T_W - T_{air}}{55.55} \right)^{1.25} \cdot \sqrt{\frac{(196.8 \cdot \upsilon_w) + 68.9}{68.9}} \right) \tag{17}$$

2. 1. 2. Combustion Sub-model According to the formulation of the indirect method (Equation (10)-(17)), it is indicated that composition and volume of flue gases were used to calculate the thermal efficiency of the fired heater. Therefore, a combustion sub-model is applied to obtain these parameters. In the combustion model, the model of complete and incomplete combustion of natural gas is proposed. Complete and incomplete combustion of natural gas can be written as Equations (18) and (19), respectively [35, 36].

$$\begin{aligned} & f_1 \cdot N_{2,fuel} + f_2 \cdot O_{2,fuel} + f_3 \cdot CO_{2,fuel} + \\ & f_4 \cdot H_2O_{fuel} + f_5 \cdot SO_{2,fuel} + f_6 \cdot CO_{fuel} + \\ & f_7 \cdot H_{2,fuel} + f_8 \cdot CH_{4,fuel} + f_9 \cdot C_2H_{4,fuel} + \\ & f_{10} \cdot C_2H_{6,fuel} + f_{11} \cdot C_3H_{8,fuel} + f_{12} \cdot C_4H_{10,fuel} + \\ & f_{13} \cdot H_2S_{fuel} + a_1 \cdot N_{2,air} + a_2 \cdot O_{2,air} \rightarrow \\ & 0.01 \cdot \left(f_1 + \left(a_1 \cdot AAS \right) \right) N_2 + 0.01 \cdot \left(a_2 \cdot \left(AAS - Air_{\min} \right) \right) O_2 \\ & + 0.01 \cdot \left(f_3 + f_6 + f_8 + 2 \cdot f_9 + 2 \cdot f_{10} + 3 \cdot f_{11} + 4 \cdot f_{12} \right) CO_2 \\ & + 0.01 \cdot \left(f_4 + f_7 + 2 \cdot f_8 + 2 \cdot f_9 + 3 \cdot f_{10} + 4 \cdot f_{11} + 5 \cdot f_{12} + f_{13} \right) H_2O \\ & + 0.01 \cdot \left(f_5 + f_{13} \right) H_2S \end{aligned} \tag{18}$$

$$\begin{aligned} & f_1 \cdot N_{2,fuel} + f_2 \cdot O_{2,fuel} + f_3 \cdot CO_{2,fuel} + f_4 \cdot H_2O_{fuel} + \\ & f_5 \cdot SO_{2,fuel} + f_6 \cdot CO_{fuel} + f_7 \cdot H_{2,fuel} + f_8 \cdot CH_{4,fuel} + \\ & f_9 \cdot C_2H_{4,fuel} + f_{10} \cdot C_2H_{6,fuel} + f_{11} \cdot C_3H_{8,fuel} + \\ & f_{12} \cdot C_4H_{10,fuel} + f_{13} \cdot H_2S_{fuel} + a_1 \cdot N_{2,air} + a_2 \cdot O_{2,air} \rightarrow \\ & 0.01 \cdot \left(f_1 + \left(a_1 \cdot AAS \right) \right) N_2 + 0.01 \cdot \left(f_5 + f_{13} \right) SO_2 + \\ & \left(\left(-AB \pm \sqrt{AB^2 - 4 \cdot AA \cdot AC} \right) / 2 \cdot AA \right) CO + \\ & \left(2 \cdot \left(a_2 \cdot \left(Air_{\min} - AAS \right) / 100 \right) \right) H_2 - \\ & \left(\left(\left(-AB \pm \sqrt{AB^2 - 4 \cdot AA \cdot AC} \right) / 2 \cdot AA \right) \right) H_2 + \\ & \left(\left(0.01 \cdot \left(f_3 + f_6 + f_8 + 2 \cdot f_9 + 2 \cdot f_{10} + 3 \cdot f_{11} + 4 \cdot f_{12} \right) \right) \right) CO_2 - \\ & \left(\left(\left(-AB \pm \sqrt{AB^2 - 4 \cdot AA \cdot AC} \right) / 2 \cdot AA \right) \right) CO_2 + \\ & \left(\left(0.01 \cdot \left(f_4 + f_7 + 2 \cdot f_8 + 2 \cdot f_9 + 3 \cdot f_{10} + 4 \cdot f_{11} + 5 \cdot f_{12} + f_{13} \right) \right) \right) H_2O - \\ & \left(\left(2 \cdot \left(a_2 \cdot \left(Air_{\min} - AAS \right) / 100 \right) \right) \right) H_2O + \\ & \left(\left(\left(-AB \pm \sqrt{AB^2 - 4 \cdot AA \cdot AC} \right) / 2 \cdot AA \right) \right) H_2O \end{aligned} \tag{19}$$

$$\begin{aligned} AB = & \left(0.01 \cdot \left(f_3 + f_6 + f_8 + 2 \cdot f_9 \right) \right) + \\ & \left(0.01 \cdot \left(2 \cdot f_{10} + 3 \cdot f_{11} + 4 \cdot f_{12} \right) \right) - \\ & \left(2 \cdot \left(a_2 \cdot \left(Air_{\min} - AAS \right) / 100 \right) \right) - \\ & \left(EC_{@TRE} \cdot \left(0.01 \cdot \left(f_4 + f_7 + 2 \cdot f_8 + 2 \cdot f_9 \right) \right) \right) - \\ & \left(EC_{@TRE} \cdot \left(0.01 \cdot \left(3 \cdot f_{10} + 4 \cdot f_{11} + 5 \cdot f_{12} + f_{13} \right) \right) \right) \\ & - \left(EC_{@TRE} \cdot \left(2 \cdot \left(a_2 \cdot \left(Air_{\min} - AAS \right) / 100 \right) \right) \right) \end{aligned} \tag{20}$$

$$AA = (1 - EC_{@TRE}) \tag{21}$$

$$AC = \left(0.01\cdot\left(f_3 + f_6 + f_8 + 2\cdot f_9\right)\right) \cdot\left(0.01\cdot\left(2\cdot f_{10} + 3\cdot f_{11} + 4\cdot f_{12}\right)\right) \cdot\left(2\cdot\left(a_2\cdot\left(Air_{\min} - AAS\right)/100\right)\right) \quad (22)$$

$$Air_{\min} = 0.01\cdot\left(0.5\cdot f_6 + 0.5\cdot f_7 + 2\cdot f_8\right) \cdot\left(3\cdot f_9 + 3.5\cdot f_{10} + 5\cdot f_{11} + 6.5\cdot f_{12} + 1.5\cdot f_{13} - f_2\right) \quad (23)$$

Moreover, EC is an equilibrium constant of following reaction and its value [35, 36].

$CO + H_2O \rightarrow CO_2 + H_2$

If surplus air is greater than or equals unity, the combustion will be complete; otherwise, combustion will be incomplete (Equation (18)).

$$Surplus = AAS\ /\ Air_{\min} \quad (24)$$

Adiabatic temperature of combustion and the actual temperature of combustion are computed as follows:

$$TAD = \frac{GCV + \left(C_{P,fuel}\cdot T_{fuel}\right) + \left(AAS\cdot C_{P,air}\cdot T_{air}\right)}{V_{fluegas}\cdot C_{P,fluegas}} \quad (25)$$

$$TRE = TAD\cdot\eta_{comb}\ /100 \quad (26)$$

2. 2. Optimization Regarding Figure 2, the GA is used to optimize the fired heater design in the present project. In this study, selected GA optimization parameters are shown in Table 1. Optimization is done with eight decision variables for the selected case study presented in Table 2. These decision variables and their range are determined based on previous research and sensitivity analysis results (section 3).

TABLE 1. Optimization conditions

Parameter	Value
crossover fraction	0.8
migration fraction	0.2
Pareto front population fraction	0.35
population size	200

TABLE 2. Decision variables for optimum design

Variables	From	To
$T_{w,o}$ [℃]	180	210
$d_{o,rad}$ [m]	0.04	0.2
$d_{o,conv}$ [m]	0.04	0.2
Nt_{rad} [-]	40	80
Nt_{radc} [-]	10	30
Excess air [-]	0.18	0.27

2. 2. 1. Objective Function As noted at the beginning of this section, the total economic and environmental cost is regarded as one of the objective functions and can be calculated as Equation (27):

$$C_{FH} = C_{rad} + C_{conv} + C_{firebox} + C_{opr} + C_{env} \quad (27)$$

where C_{rad}, C_{conv}, $C_{firebox}$, C_{opr}, and C_{env} correspond to the cost of radiation section, convection section, firebox, operation, and environmental emission, respectively.

$$C_{rad} = r_{cost}\cdot A_{cp}\cdot CRF \quad (28)$$

$$C_{conv} = c_{cost}\cdot A_{conv}\cdot CRF \quad (29)$$

where c_{cost} refers to unitary cost.

$$C_{firebox} = \left[k_1 + k_2\left(A_{conv} + A_{cp}\right)\right]\cdot CRF \quad (30)$$

where k_1 and k_2 correspond to constants required for computing costs.

$$C_{opr} = \left(o_{\text{cost}}\cdot m_{fuel}\right)\cdot h + \left(\frac{c_{ele}}{\eta_p}\left(\frac{m_w}{\rho_w}\cdot\frac{0.00517\cdot f\cdot v\cdot G^2\cdot L_e}{d_i}\right)\right)\cdot h \quad (31)$$

where c_{ele}, o_{cost}, and h are considered to be €0.01/kWh [37], €0.01/m^3 [38], and 7000 h, respectively. Finally, the cost of emission is calculated as follows:

$$C_{env} = \left[\left(m_{CO_2}\cdot c_{CO_2}\right) + \left(m_{SO_2}\cdot c_{SO_2}\right)\right]\cdot h \quad (32)$$

The values of m_{CO_2} and m_{SO_2} are obtained using the combustion sub-model (Section 2.1.2). The values of c_{CO_2} and c_{SO_2} are \$0.032/kg, and \$2.227/kg, respectively [39].

Modified exergy efficiency is considered to be another objective function and is obtained as Equation (33):

$$\eta_{exe} = \frac{Ex_P}{Ex_F - Ex_D^{UN}} \quad (33)$$

where Ex_P and Ex_F refer to product exergy (absorbed exergy from water stream) and fuel exergy, respectively and are computed as Equations (34) and (35) [40]:

$$Ex_P = m_w\left[\left(h_{w,o} - h_{w,i}\right) - T_0\left(S_{w,o} - S_{w,i}\right)\right] \quad (34)$$

$$Ex_F = \xi\cdot m_{fuel}\cdot LHV - Ex_{flue} \quad (35)$$

ξ is a constant value to calculate the exergy efficiency of fuel. The value of this parameter for gas fuel is 0.98

[40]. Equation (36) is applied to achieve exergy of flue gas. The combustion sub-model was implemented to obtain the composition and molar fraction of flue gases.

$$Ex_{flue} = m_{flue} \cdot (ex^{ph}_{flue} + ex^{ch}_{flue}) \quad (36)$$

$$ex^{ph}_{flue} = \sum_k \left(h_k - h_{0,k}\right) - T_0 \left(s_k - s_{0k}\right) \quad (37)$$
$$k = N_2, O_2, CO_2, CO, SO_2, H_2O$$

$$ex^{ch}_{flue} = n.\left(\sum_k x_k \cdot e^{ch}_k + \bar{R} T_0 \sum_k x_k \ln\left(x_k\right)\right) \quad (38)$$
$$k = N_2, O_2, CO_2, CO, SO_2, H_2O$$

The standard mole chemical exergy of components is presented in Table 3. Unavoidable exergy destruction of the fired heater is calculated as follows:

$$Ex^{UN}_{D,FH} = Ex_{P,FH}\left(\frac{Ex_{D,FH}}{Ex_{P,FH}}\right)^{UN} \quad (39)$$

To determine the value of $\left(Ex_{D,FH}/Ex_{P,FH}\right)^{UN}$, it is assumed that the minimum temperature difference of HE is 5 K, isentropic efficiency of the pump is 0.95, air and fuel temperature are 673 K, and excess air is 0.12.

2. 3. Case study The heater of the Ramin Power Plant gas reduction station in Iran was selected as a case study in the present research work [41]. As already stated earlier, this heater is used to preheat the natural gas before entering the expansion turbine, which is parallel to the pressure regulator whose purpose is power generation. Heat transfer value, required on the coldest day of the year to preheat the natural gas, is considered the heat transfer rate. The hot fluid is water. Figure 3 depicts a configuration of natural gas pressure reduction station applying turboexpander as well as a fired heater. The properties of the natural gas in natural gas reduction station of the Ramin power plant, regarded as input variables in the mathematical model, are presented in Table 4.

TABLE 3. Standard chemical molar exergy of flue gas components [40]

Substance	e^{ch} [J/mol]
N_2	584
O_2	3869
CO_2	19870
H_2O	9490
CO	275100
SO_2	313400

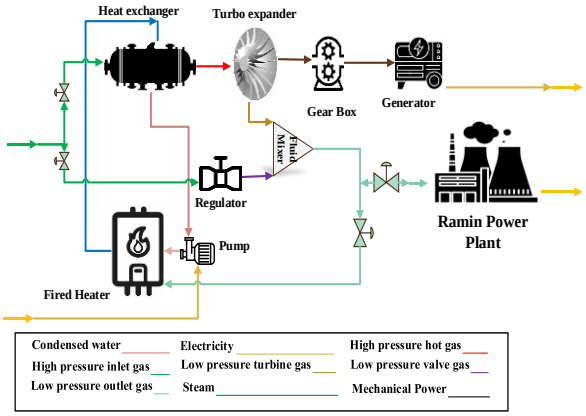

Figure 3. Configuration of power plant natural gas pressure reduction station using turboexpander and hot water GFH

TABLE 4. Dataset for the design of heater [41]

Parameter		Value
m_{ng} [kg/s]		32.83
$T_{ng,i}$ [K]		288.8
$T_{ng,o}$ [K]		388.2
Compositions (volume fraction) [%]	N_2	1.735
	CO_2	3.52
	CH_4	80.43
	C_2H_4	1.5
	C_2H_6	9.02
	C_3H_8	4.54
	C_4H_{10}	0.58
	H_2S	0.09

3. RESULTS AND DISCUSSION

3. 1. Model Validation In this section, the validity and accuracy of the developed model are considered to be examined. The answer reached for the model is compared with the Ibrahim and Al-Qassimi Design [17]. To do so, input variables of design model such as outlet hot water temperature, the external diameter of tube in radiation as well as convection sections, number of the wall-side tube as well as the ceiling in radiation section, excess air ratio, natural gas composition, air humidity ratio, relative effectiveness factor of the tubes bank, and air as well as fuel temperature are collected form this study [17]. As shown in Table 5, there is a plausible difference between the two results, so the proposed model can be successfully used with satisfactory

accuracy. The heat liberated by combustion has the maximum deviation. It results from considering the indirect method of estimating efficiency due to the capability of the combustion model to obtain the composition of flue gases. Design models of fired heaters include thermodynamic and geometrical equations and performance prediction equations (section 2.1.1). These models yield design, thermodynamic and performance parameters of the fired heater through an iterative process (see Figure 2). To evaluate applying indirect method for estimating heater efficiency, the thermal efficiency of mentioned gas-fired heater [17] is calculated and compared with that of experimental methods proposed by previous design models [26, 28], which is presented in Table 6. In these studies [26, 28], the thermal efficiency of the fired heater is calculated using the direct method, which depends on stack temperature and excess air fraction. To do so, the mathematical model of fired heater (section 2.1.1) and direct method equations for calculating thermal efficiency are used to obtain the design and performance parameters of the fired heater. Compared to previous estimation methods [26, 28], the indirect method gives the best prediction with a deviation of 2.22% from experimental values.

TABLE 5. Model validation

Variables	Ref. [17]	This study	Deviation [%]
T_g [K]	1073	1070	**0.28**
T_s [K]	673	675	**0.3**
$T_{w,i,rad}$ [K]	516	523	**1.4**
Q_f [kW]	31091.6	34816	**11.9**
Q_{rad} [kW]	17172.2	16813	**2**
Q_{conv} [kW]	6388.8	6693.2	**4.76**
$N_{t,total}$ [-]	100	110	**10**
$N_{t,shld}$ [-]	8	8	**0**
W [m]	4.8	5.1	**6**
L [m]	20	19.3	**3.5**

TABLE 6. Comparison of various methods to estimate thermal efficiency of fired heater

Variables	Ibrahim Design [17]	Mussati Method [26] (Dev. From [17])	Bahadori Method [28] (Dev. From [17])	This study (Dev. From [17])
η_{FH} [%]	0.7578	0.815 (**5.72 %**)	0.722 (**3.58 %**)	**0.78 (2.22 %)**

3. 2. Optimization Results and Parametric Analysis The Pareto front curve obtained from the optimization using total economic and environmental cost, and modified exergy efficiency (optimal design I) is depicted in Figure 4. According to this figure, an increase in the modified exergy efficiency can lead to a rise in the total cost. The highest modified exergy efficiency is 0.5213, resulting in a total economic and environmental cost of $587053.56, which has the highest value. The lowest modified exergy efficiency belongs to 0.487, with the minimum cost of $ 529919.9. To provide valuable insight into the fired heater's multi-optimal design, Pareto-front fitted curve is shown in Figure 4. The LINMAP optimal point marks in Figure 4.

To evaluate proposed objective functions (optimal design I), optimization using thermal efficiency with total economic and environmental cost (optimal design II) as objective functions was implemented, see Figure 5. Characteristics values of LINMAP suggested point of optimal design I is represented and compared with those of optimal design II in Table 7.

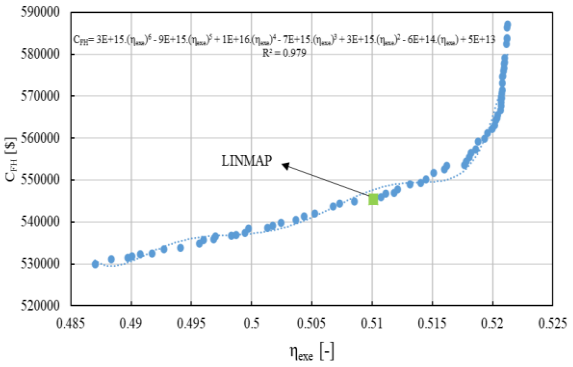

Figure 4. Pareto-front curve for optimization of modified exergy efficiency versus total cost (optimal design I)

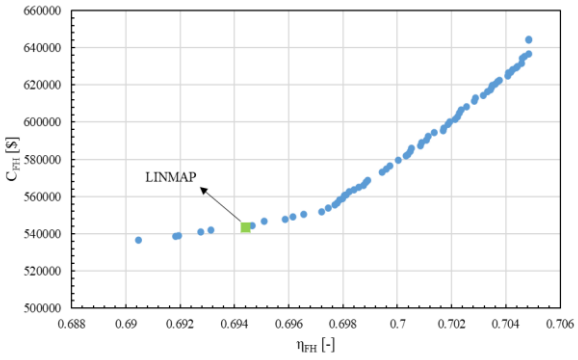

Figure 5. Pareto-front curve for optimization of energy efficiency versus total cost (optimal design II)

TABLE 7. Specifications of the LINMAP suggested points indicated in the Pareto front curves

	Parameters	LINMAP	
		Optimal design I	Optimal design II
Decision variables	$T_{w,o}$ [°C]	195.4	180.1
	$d_{o,rad}$ [m]	0.04	0.0401
	$d_{o,conv}$ [m]	0.1128	0.1317
	$N_{t,rad}$ [-]	40	63
	$N_{t,radc}$ [m]	10	13
	Excess air [-]	0.2227	0.2442
Objective functions	C_{FH} [$]	545370.7	543245.9
	η_{exe} [-]	0.5101	0.4971
	η_{FH} [-]	0.731	0.6944
Design parameters	Q_{rad} [MW]	3.788	4.223
	Q_{conv} [MW]	1.957	1.739
	Q_{shld} [MW]	2.109	1.8929
	A_{cp} [m^2]	45.3612	64.9357
	A_{conv} [m^2]	69.4182	77.5283
	$N_{t,conv}$ [-]	24	23
	ΔP_t [Pa]	31374	17864.5
	T_g [K]	1172.5	1103.4
	V [m^3]	76.46	152.56
	m_{fuel} [kg/s]	0.2448	0.2574

According to Table 7, LINMAP suggested point in optimal design I has a higher total cost (0.4%) and modified exergy efficiency (1.3%) than LINMAP suggested point in optimal design II. It results from a considerable reduction in total heat exchanger area (because of reduction in tube length in radiation section, external tube diameter in convection section, number of tubes in radiation section, and number of tubes in convention section), and a rise in effective gas temperature in firebox (T_g).

The heat exchanger area in LINMAP suggested optimal design I decreases in contrast to optimal design II due to reduction in the number of tubes. Furthermore, employing modified exergy efficiency, and total economic and environmental cost as objective functions (optimal design I) results in smaller heat transfer area of radiation zone with a lower number of tubes compared to results of optimal design II, which causes a decrease in investment cost [26]. As mentioned in the methodology section, heat demand is assumed to be constant; therefore, excess air decreases and effective gas temperature in the firebox increases to compensate for the reduction in total heat exchanger area compared with optimal design II. Moreover, a decrease in excess air of LINMAP suggested points of optimal design I leads to improvement in energy efficiency in contrast to that of optimal design II [42]. The total pressure drop of the tube-side of the fired heater increases significantly due to a reduction in external tube diameter in the convection section, which is in line with previous studies [27]. It should be mentioned that allowable pressure drop of tube-side is considered1000 kPa [43].

For sensitivity analysis, the effects of key parameters, namely hot water outlet temperature, the external diameter of the tube in radiation as well as convection sections, number of side-wall as well as ceiling tube in radiation section, and excess air ratio are investigated on objective functions and presented in Figures 6 to 10, respectively. In this study, the LINMAP optimal point considered as a reference point. According to these figures, hot water outlet temperature is employed along with other decision variables due to the remarkable effects of this parameter on objective functions. According to Figure 6, an increase in the tube's external diameter in the radiation section raises total cost due to an increase in the total heat exchanging area. However, with increasing this parameter, modified exergy efficiency remains unchanged at low values of hot water outlet temperature. At high values of hot water outlet temperature, modified exergy efficiency first increases then decreases. An increase in hot water outlet temperature leads to rise in modified exergy efficiency at low values of external diameters of the tube. However, it fluctuates slightly at high values of external diameter, which results from large changes in the mean heat flux of large diameter tubes because of a lower degree of shadowing in these tubes [44].

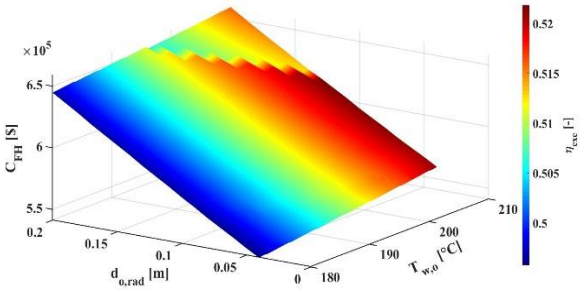

Figure 6. The effect of water outlet temperature and external diameter of tube in radiation section on modified exergy efficiency and total cost

Figure 7 reveals a surface plot of modified exergy, and total economic and environmental cost of fired heater versus external diameter of tube in convention section and hot water outlet temperature. An increase in external diameter of tube in convention section increases total cost, but it causes an initial climb in modified exergy efficiency, decreasing afterwards. It can be seen that a rise in hot water outlet temperature increases total economic and environmental cost at low values of the external diameter of the convention tube. However, it leads to a reduction in total cost at high values of the external diameter of the convention tube. Moreover, it is indicated that the diameter of tube in the radiation section (Figure 6) has a greater impact on total cost than the diameter of tube in the convection section, which concurs with previous research [27].

Figure 8 indicates that the total cost of the fired heater increases gradually by increasing either the number of the side-wall tubes in the radiation section or hot water outlet temperature. The number of the side-wall tubes has no considerable effect on modified exergy efficiency.

According to Figure 9, the effects of the number of the ceiling tubes in the radiation section on total cost and modified exergy efficiency bear a close resemblance to those of the number of the side-wall tubes (Figure 8).

Figure 10 provides an assessment of the total economic and environmental cost, and modified exergy efficiency of the fired heater for excess air and hot water outlet temperature. An increase in excess air leads to a slight rise in the total cost and a small drop in modified exergy efficiency. These results match those observed in previous studies [28, 45]. The latter result is a narrower recirculation zone and a larger vortex shedding upward in the combustion zone with an increase in excess air [45].

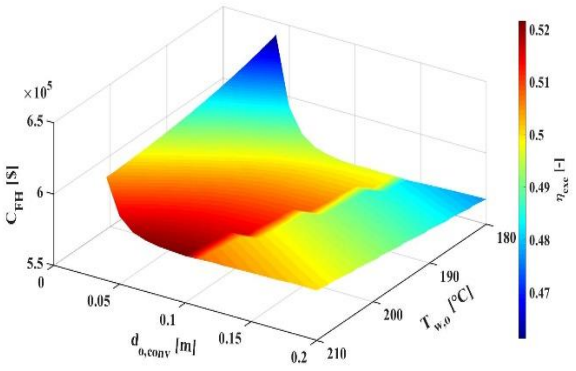

Figure 7. The effect of water outlet temperature and external diameter of tube in convection section on modified exergy efficiency and total cost

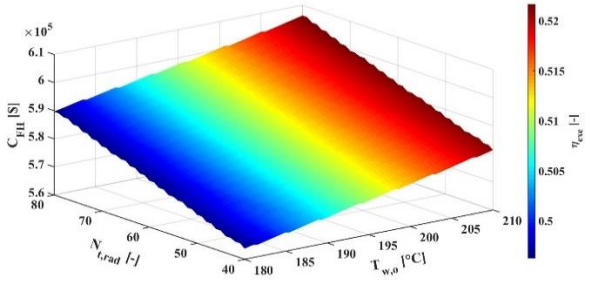

Figure 8. The effect of water outlet temperature and number of side-wall tube in radiation section on modified exergy efficiency and total cost

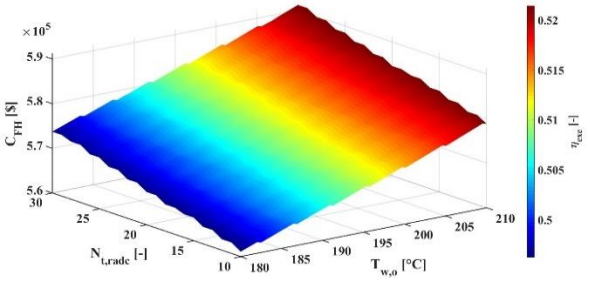

Figure 9. The effect of water outlet temperature and number of ceiling tube in radiation section on modified exergy efficiency and total cost

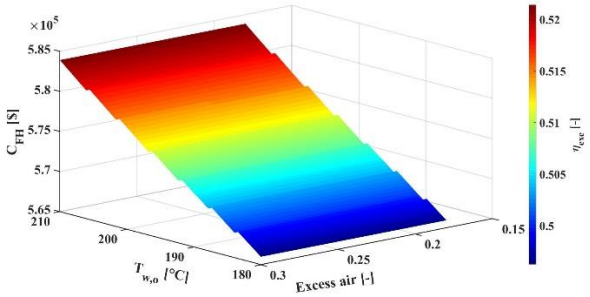

Figure 10. The effect of water outlet temperature and excess air on modified exergy efficiency and total cost

4. CONCLUSIONS

The present study puts forward a fired heater design model integrated with a combustion sub-model to optimize the fired heater. A multi-objective optimization of the fired heater in a natural gas pressure reducing station is carried out using a genetic algorithm. In this regard, the mathematical model of fired heater and sub-model of combustion are developed to achieve design and performance parameters of the fired heater. LINMAP method is applied to suggest an optimal solution between Pareto-set points. The hot water outlet temperature, the external diameter of tubes in radiation

and convection sections, the number of side-wall and ceiling tubes in the radiation section, and excess air ratio are selected as design parameters. Finally, sensitivity analysis of design parameters and their effects on objective functions are performed individually. According to the results, the developed model enables a more accurate prediction of heaters' thermal efficiency compared with previous models. LINMAP yielded a solution for optimization using modified exergy efficiency and total cost as objective functions leading to an increase of 0.4% in total cost and 1.3% in modified exergy efficiency compared with that of optimization applying thermal efficiency and total cost as objective functions, respectively.

As noted in the introduction section, Iran has 2500 gas reduction stations, which traditionally consist of the gas-fired heater, throttling valve, heat exchanger, and control system. Moreover, fired heaters burn a significant portion of the passing natural gas, and have low energy efficiency. Therefore, the results of this study can be applied to assess the potential of energy and natural gas consumption savings in gas reduction stations in Iran.

It is also indicated in the introduction section that renewable heating systems and novel-heating technologies are not cost-effective solutions. Considering pollution cost is known as one of the main solutions to face mentioned challenges, and it should be considered in the optimal design of gas-fired heaters to move toward and develop efficient and low emission heating systems. Therefore, this study can be compared with future studies on applying renewable heating systems in natural gas stations in Iran. In our future research, we intend to focus on the optimal design of the gas reduction station system considering all components of the system, including heat exchanger, heater, turbo-expander, and throttle valve. System restrictions will also be taken into account to determine and propose a set of practical recommendations.

5. APPENDIX A

At first, objective functions should be non-dimensionalized, applying Euclidian non-dimensionalization, due to different dimensions of objective functions on the Pareto frontier [34].

$$F_{ij}^{n} = \frac{F_{ij}}{\sqrt[2]{\sum_{i=1}^{m}\left(F_{ij}\right)^{2}}} \quad \text{(A.1)}$$

Then the distance of each point on the Pareto frontier from ideal point (F_j^{ideal}) in which each objective has its best value, is calculated as follows [34]:

$$d_{i+} = \sqrt[2]{\sum_{j=1}^{n}\left(F_{ij} - F_j^{ideal}\right)^{2}} \quad \text{(A.2)}$$

LINMAP suggested solution is a point with a minimum distance from the ideal point.

6. REFERENCES

1. Dudley, B., *Bp statistical review of world energy*, in *BP Statistical Review, London, UK, accessed Aug*. 2018.116.
2. Daneshi, H., Zadeh, H.K. and Choobari, A.L., "Turboexpander as a distributed generator", in 2008 IEEE Power and Energy Society General Meeting-Conversion and Delivery of Electrical Energy in the 21st Century, Pittsburgh, PA, USA, IEEE., (2008), 1-7.
3. Farzaneh-Gord, M., Arabkoohsar, A., Dasht-bayaz, M.D., Machado, L. and Koury, R., "Energy and exergy analysis of natural gas pressure reduction points equipped with solar heat and controllable heaters", ***Renewable Energy***, Vol. 72, (2014), 258-270.
4. Olfati, M., Bahiraei, M., Heidari, S. and Veysi, F., "A comprehensive analysis of energy and exergy characteristics for a natural gas city gate station considering seasonal variations", ***Energy***, Vol. 155, (2018), 721-733.
5. Bloch, H. and Soares, C., "Turboexpanders and process applications, Gulf Professional Publishing, (2001).
6. Požívil, J., "Use of expansion turbines in natural gas pressure reduction stations", ***Acta Montanistica Slovaca***, Vol. 3, No. 9, (2004), 258-260.
7. Ashouri, E., Veysi, F., Shojaeizadeh, E. and Asadi, M., "The minimum gas temperature at the inlet of regulators in natural gas pressure reduction stations (CGS) for energy saving in water bath heaters", ***Journal of Natural Gas Science and Engineering***, Vol. 21, (2014), 230-240.
8. Soleimani, P., Khoshvaght-Aliabadi, M., Rashidi, H. and Bahmanpour, H., "Performance enhancement of water bath heater at natural gas city gate station using twisted tubes", ***Chinese Journal of Chemical Engineering***, Vol. 28, No. 1, (2020), 165-179.
9. Arabkoohsar, A., Farzaneh-Gord, M., Deymi-Dashtebayaz, M., Machado, L. and Koury, R., "A new design for natural gas pressure reduction points by employing a turbo expander and a solar heating set", ***Renewable Energy***, Vol. 81, (2015), 239-250.
10. Ghezelbash, R., Farzaneh-Gord, M., Behi, H., Sadi, M. and Khorramabady, H.S., "Performance assessment of a natural gas expansion plant integrated with a vertical ground-coupled heat pump", ***Energy***, Vol. 93, No., (2015), 2503-2517.
11. Bargiel, P., Kostowski, W. and Usón, S., "An approach to enhance combined cycle performance by integration with a gas pressure reduction station", ***Journal of Power Technologies***, Vol. 95, No. 1, (2015).
12. Farzaneh-Kord, V., Khoshnevis, A., Arabkoohsar, A., Deymi-Dashtebayaz, M., Aghili, M., Khatib, M., Kargaran, M. and Farzaneh-Gord, M., "Defining a technical criterion for economic justification of employing chp technology in city gate stations", ***Energy***, Vol. 111, (2016), 389-401.
13. Arabkoohsar, A., Gharahchomaghloo, Z., Farzaneh-Gord, M., Koury, R. and Deymi-Dashtebayaz, M., "An energetic and economic analysis of power productive gas expansion stations for employing combined heat and power", ***Energy***, Vol. 133, (2017), 737-748.

14. Darabi, A., Shariati, A., Ghanaee, R. and Soleimani, A., "Economic assessment of a hybrid turboexpander-fuel cell gas energy extraction plant", ***Turkish Journal of Electrical Engineering & Computer Sciences***, Vol. 24, No. 3, (2016), 733-745.
15. Saadat-Targhi, M. and Khanmohammadi, S., "Energy and exergy analysis and multi-criteria optimization of an integrated city gate station with organic rankine flash cycle and thermoelectric generator", ***Applied Thermal Engineering***, Vol. 149, (2019), 312-324.
16. Farzaneh-Gord, M., Arabkoohsar, A., Dasht-bayaz, M.D. and Farzaneh-Kord, V., "Feasibility of accompanying uncontrolled linear heater with solar system in natural gas pressure drop stations", ***Energy***, Vol. 41, No. 1, (2012), 420-428.
17. Ibrahim, H.A.-H. and Al-Qassimi, M., "Simulation of heat transfer in the convection section of fired process heaters", ***Periodica Polytechnica Chemical Engineering***, Vol. 54, No. 1, (2010), 33-40.
18. Association, G.P.S., "Engineering data book, Gas Processors Suppliers Association, (2004).
19. Sinnott, R., "Chemical engineering design, Elsevier, (2014).
20. Ebrahimi, H., Mohammadzadeh, J.S.S., Zamaniyan, A. and Shayegh, F., "Effect of design parameters on performance of a top fired natural gas reformer", ***Applied Thermal Engineering***, Vol. 28, No. 17-18, (2008), 2203-2211.
21. Hottel, H. and Cohen, E., "Radiant heat exchange in a gas-filled enclosure: Allowance for nonuniformity of gas temperature", ***AIChE Journal***, Vol. 4, No. 1, (1958), 3-14.
22. Ibrahim, H.A.-H. and Al-Qassimi, M., "Matlab program computes thermal efficiency of fired heater", ***Periodica Polytechnica Chemical Engineering***, Vol. 52, No. 2, (2008), 61-69.
23. Towler, G. and Sinnott, R., "Chemical engineering design: Principles, practice and economics of plant and process design, Elsevier, (2012).
24. Institute, A.P., *Standard 530: Calculation of heater tube thickness in petroleum refineries*. 2008, Washington, DC: American Petroleum Institute.58.
25. Institute, A.P., *Standard 560: Fired heaters for general refinery services*. 2001, Washington, DC: American Petroleum Institute.
26. Mussati, S., Manassaldi, J.I., Benz, S.J. and Scenna, N.J., "Mixed integer nonlinear programming model for the optimal design of fired heaters", ***Applied Thermal Engineering***, Vol. 29, No. 11-12, (2009), 2194-2204.
27. Haratian, M., Amidpour, M. and Hamidi, A., "Modeling and optimization of process fired heaters", ***Applied Thermal Engineering***, Vol. 157, No., (2019), 113722.
28. Bahadori, A. and Vuthaluru, H.B., "Novel predictive tools for design of radiant and convective sections of direct fired heaters", ***Applied Energy***, Vol. 87, No. 7, (2010), 2194-2202.
29. Abdolalipouradl, M., Khalilarya, S. and Jafarmadar, S., "Energy and exergy analysis of a new power, heating, oxygen and hydrogen cogeneration cycle based on the sabalan geothermal wells", ***International Journal of Engineering***, ***Transactions C: Aspects,*** Vol. 32, No. 3, (2019), 445-450.
30. Dincer, I. and Rosen, M.A., "Exergy: Energy, environment and sustainable development, Newnes, (2012).
31. Kazemzadeh Hannani, S., Saidi, M. and Jafarian, A., "Second law based analysis of fluid flow in the regenerator of pulse tube refrigerators", ***International Journal of Engineering***, ***Transactions A: Basics,*** Vol. 21, No. 2, (2008), 181-194.
32. Rath, M. and Acharya, S., "Exergy and energy analysis of diesel engine using karanja methyl ester under varying compression ratio", ***International Journal of Engineering***, ***Transactions B: Applications,*** Vol. 27, No. 8, (2014), 1259-1268.
33. Lemmon, E.W., Huber, M.L. and McLinden, M.O., *Nist standard reference database 23: Reference fluid thermodynamic and transport properties-refprop*, in *NIST standard reference database*. 2013.
34. Sayyaadi, H. and Mehrabipour, R., "Efficiency enhancement of a gas turbine cycle using an optimized tubular recuperative heat exchanger", ***Energy***, Vol. 38, No. 1, (2012), 362-375.
35. Ismail, O.S. and Umukoro, G.E., "Modelling combustion reactions for gas flaring and its resulting emissions", ***Journal of King Saud University-Engineering Sciences***, Vol. 28, No. 2, (2016), 130-140.
36. Turns, S.R., "Introduction to combustion, McGraw-Hill Companies, (1996).
37. Ministry, P., *Electricity tariffs and their general conditions from the beginning of may, 2019*. 2019.11.
38. Ministry, P., *Natural gas tariffs*. 2020.2.
39. He, L., Lu, Z., Pan, L., Zhao, H., Li, X. and Zhang, J., "Optimal economic and emission dispatch of a microgrid with a combined heat and power system", ***Energies***, Vol. 12, No. 4, (2019), 604.
40. Frangopoulos, C.A., "Exergy, energy system analysis and optimization-volume iii: Artificial intelligence and expert systems in energy systems analysis sustainability considerations in the modeling of energy systems, EOLSS Publications, Vol. 3, (2009).
41. Pakzad, A., "Turboexpanders and energy recovery", 1 st ed, Tehran, Iran, Afrooz Publishing, (2010), 350.
42. Stehlik, P., Kohoutek, J. and Jebáček, V., "Simple mathematical model of furnaces and its possible applications", ***Computers & Chemical Engineering***, Vol. 20, No. 11, (1996), 1369-1372.
43. Shekarchian, M., Zarifi, F., Moghavvemi, M., Motasemi, F. and Mahlia, T., "Energy, exergy, environmental and economic analysis of industrial fired heaters based on heat recovery and preheating techniques", ***Energy Conversion and Management***, Vol. 71, (2013), 51-61.
44. Hájek, J. and Jegla, Z., "Standards for fired heater design: Analysis of two dominant heat flux variation factors", ***Applied Thermal Engineering***, Vol. 125, (2017), 702-713.
45. Khodabandeh, E., Pourramezan, M. and Pakravan, M.H., "Effects of excess air and preheating on the flow pattern and efficiency of the radiative section of a fired heater", ***Applied Thermal Engineering***, Vol. 105, (2016), 537-548.

Persian Abstract

چکیده

در این پژوهش، مدلی جدید به منظور طراحی بهینه گرمکن آب داغ با لحاظ کردن مدل احتراق ارائه شد. مدل توسعه یافته توانایی طراحی تمامی بخش های گرمکن آب داغ از قبیل محفظه تشعشعی، بخش همرفت و بخش محافظ و همچنین محاسبه ترکیبات و حجم گازهای حاصل از احتراق را دارد. طراحی بهینه چندهدفه گرم کن آب داغ ایستگاه تقلیل فشار گاز نیروگاه رامین بر مبنای مدل توسعه یافته انجام شد. هزینه کل اقتصادی و زیست محیطی همراه با بازدهی اگزرژی اصلاحی به عنوان توابع هدف در نظر گرفته شدند. علاوه براین، روش تصمیم گیری چند معیاره به منظور پیشنهاد نقطه بهینه از بین نقاط بهینه نمودار پرتو بهینه سازی چند هدفه استفاده شد. مدل توسعه یافته جدید عملکرد بهتری در پیش بینی بازدهی گرم کن آب داغ نسبت به مدل های پیشین دارد. نتایج بهینه سازی نشان داد که نقطه بهینه پیشنهادی روش تصمیم گیری چندمعیاره لینمپ بر مبنای توابع هدف پیشنهادی نسبت به نقطه مشابه بهینه سازی بر مبنای توابع هدف اقتصادی و بازدهی انرژی، بازدهی اگزرژی بیشتری دارد (۱/۳ ٪) در حالی که هزینه کل ثابت باقی می ماند. در نهایت، تأثیر هر یک از متغیرهای تصمیم گیری بهینه سازی بر توابع هدف مورد ارزیابی قرار گرفت.